

# Transformation of external-ear spectral cues into perceived delays by the big brown bat, *Eptesicus fuscus*

James A. Simmons<sup>a)</sup>

Department of Neuroscience, Brown University, Providence, Rhode Island 02912

Janine M. Wotton and Michael J. Ferragamo

Biology Department, Gustavus Adolphus College, St. Peter, Minnesota 56082

Cynthia F. Moss

Department of Psychology, University of Maryland, College Park, Maryland 20742

(Received 16 February 2000; revised 28 January 2002; accepted 1 February 2002)

The external-ear transfer function for big brown bats (*Eptesicus fuscus*) contains two prominent notches that vary from 30 to 55 kHz and from 70 to 100 kHz, respectively, as sound-source elevation moves from  $-40$  to  $+10$  degrees. These notches resemble a higher-frequency version of external-ear cues for vertical localization in humans and other mammals. However, they also resemble interference notches created in echoes when reflected sounds overlap at short time separations of 30–50  $\mu$ s. Psychophysical experiments have shown that bats actually perceive small time separations from interference notches, and here we used the same technique to test whether external-ear notches are recognized as a corresponding time separation, too. The bats' performance reveals the elevation dependence of a time-separation estimate at 25–45  $\mu$ s in perceived delay. Convergence of target-shape and external-ear cues onto echo spectra creates ambiguity about whether a particular notch relates to the object or to its location, which the bat could resolve by ignoring the presence of notches at external-ear frequencies. Instead, the bat registers the frequencies of notches caused by the external ear along with notches caused by the target's structure and employs spectrogram correlation and transformation (SCAT) to convert them all into a family of delay estimates that includes elevation. © 2002 Acoustical Society of America.

[DOI: 10.1121/1.1466869]

PACS numbers: 43.66.Gf, 43.66.Mk, 43.80.Lb [WA]

## I. INTRODUCTION

Echolocating big brown bats (*Eptesicus fuscus*) transmit wideband, frequency-modulated (FM) biosonar sounds covering frequencies roughly from 20 to 100 kHz and perceive objects from echoes of these sounds returning to the ears (Griffin, 1958; Popper and Fay, 1995). These bats employ sonar for orientation in a surprisingly wide variety of situations (Simmons *et al.*, 2001). The bat's primary perceptual dimension for registering objects is target range from the delay of FM echoes (Simmons, 1973, 1980, 1989). Behavioral experiments have established that these bats remember an "image" (for sense of term, see Simmons, 1989) consisting of an estimate for the delay of each replica of the broadcast included in a cluster of reflections (Simmons *et al.*, 1995). Here, we examine how the acoustic properties of the bat's external ears contribute one component to this delay image.

Big brown bats receive FM echoes with an integration-time of about 300–400  $\mu$ s, probably originating in the bandpass and lowpass filter stages involved in auditory transduction (Simmons *et al.*, 1989) and carried over in recovery times of neural responses in the auditory brainstem (reviewed by Casseday and Covey, 1995; Pollak and Casseday, 1989). Two reflected replicas of the broadcast arriving closer

together than this integration-time merge into a single sound for purposes of detection. However, the bat's FM sounds are several milliseconds long, whereas the integration-time is less than half a millisecond, so the echo waveforms can overlap and still be detected as separate FM sweeps. Consequently, the bat's internal representation of FM echoes must be shorter than the sounds themselves. This representation takes the form of an auditory spectrogram made up of segments of the FM sweeps segregated by the bandpass filters in the cochlea and the excitatory tuning curves of auditory neurons (Simmons *et al.*, 1996). To the bat, overlap of two echoes only occurs when their respective spectrograms merge at a time separation of 300–400  $\mu$ s (Saillant *et al.*, 1993; Simmons *et al.*, 1989).

Reflections from multiple glints interfere with each other if they are closer together than the integration-time, and the resulting modulation of the echo spectrum affects the performance of bats in psychophysical discrimination experiments (Mogdans and Schnitzler, 1990; Schmidt, 1992; Simmons *et al.*, 1989). The spectrogram created by interference contains peaks and notches in amplitude at specific frequencies according to the time-separation of the reflections (see Beuter, 1980; Dear *et al.*, 1993; Mogdans and Schnitzler, 1990; Schmidt, 1992; Saillant *et al.*, 1993). These notches are the most prominent features of the interference spectrum (Altes, 1984). For echoes arriving in the same phase, notches are

<sup>a)</sup>Electronic mail: james\_simmons@brown.edu

## INTERFERENCE NOTCHES FOR GLINTS

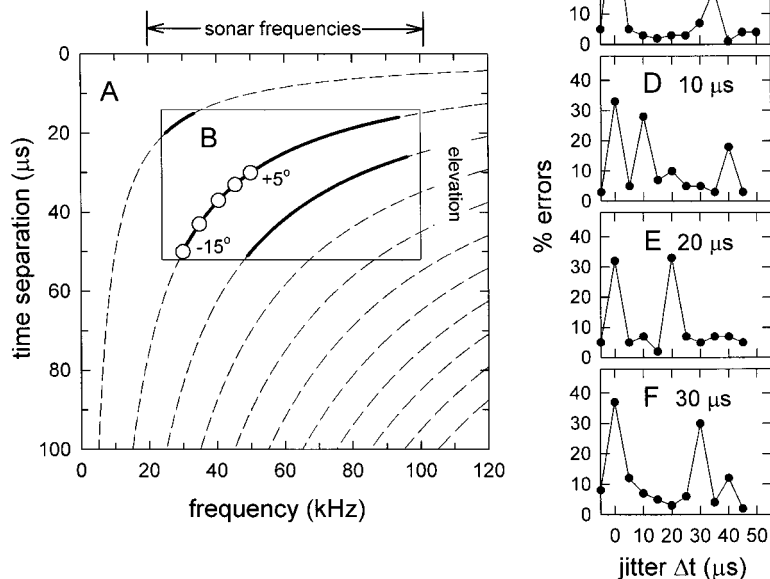


FIG. 1. (a) Family of curves tracing the relation between the time separation of two overlapping echoes in  $\mu\text{s}$  and the frequencies of interference notches (dashed curves). Counting the lines from left to right, they correspond to  $n=0,1,2,\dots,10,11$  in Eq. (1). (b) Inset showing relation between sound-source elevation and frequencies of interference notches (solid curves superimposed on dashed curves) in the bat's external-ear transfer function (data-points from  $+5$  to  $-15$  degrees from Fig. 2). (c) Percentage errors obtained from a big brown bat in the jittered echo experiment with single-glitter replicas of the broadcast for simulated echoes *a* and *b* [Simmons *et al.*, 1990b; see also Figs. 4(b), (e), and (h)]. The secondary error peak in the curve (arrow) at  $35 \mu\text{s}$  is the focus of the present experiments. (d)–(f) Percentage errors obtained from the same bat in the jittered echo experiment with overlapping two-glitter replicas of the broadcast for simulated echo *a* at time separations of 10, 20, or 30  $\mu\text{s}$  (Simmons, 1993). Error peak at 0  $\mu\text{s}$  corresponds to the arrival-time of simulated echoes from the first glint, while peaks at 10  $\mu\text{s}$  (d), 20  $\mu\text{s}$  (e), or 30  $\mu\text{s}$  (f) correspond to the arrival-time of simulated echoes from the second glint.

located at odd-harmonic frequencies ( $f_n$ , in ratios of 1,3,5...) given by Eq. (1):

$$f_n = (2n + 1)/2t_s, \quad \text{where } n = 0, 1, 2, 3, \dots \quad (1)$$

Figure 1(a) plots the frequencies of interference notches for echo time separations from 0 to 100  $\mu\text{s}$ . As delay separation increases (downward on vertical axis), the frequencies of particular notches become lower (leftward on horizontal axis), and the frequency spacing of neighboring notches becomes smaller (frequency spacing is the reciprocal of the time separation). For example, at a time separation of 10  $\mu\text{s}$  there is just one notch at 50 kHz, but at a time separation of 20  $\mu\text{s}$  there are two notches at 25 and 75 kHz, and at a time separation of 40  $\mu\text{s}$  there are numerous notches at 12.5, 37.5, 62.5, 87.5, and 112.5 kHz. The big brown bat can directly detect only those notches that are included in its sonar frequencies [top of Fig. 1(a)].

One interpretation of Fig. 1(a) is that interference notches provide useful timbre-like “spectral coloration” to echoes from complex objects (Neuweiler, 2000; Schmidt, 1992). FM bats are capable of discriminating between targets of different shape or texture whose echoes differ in their interference spectra (Bradbury, 1970; Griffin, 1967; Haber-setzer and Vogler, 1983; Schmidt, 1988; Simmons *et al.*, 1974). However, consideration of the acoustic origin for this spectral coloration (see Simmons and Chen, 1989) has raised the possibility that FM bats might perceive not merely the coloration but instead the time-separation between overlapping reflections—that is, the glints themselves (Simmons, 1980). Several different psychophysical experiments have demonstrated unequivocally that the big brown bat indeed does perceive and, crucially, *remember* the arrival-times of each of the broadcast replicas embedded in the compound reflection from multiple glints. In an ordinary echo-delay discrimination procedure, big brown bats remember the delay for both the first and the second of two echoes only 100  $\mu\text{s}$

apart (Simmons *et al.*, 1990a). In a more sensitive procedure employing jittered echoes, bats remember the delays of both the first and the second echoes at separations of 10, 20, and 30  $\mu\text{s}$  (Saillant *et al.*, 1993; Simmons, 1993). These separations are all well inside the 300–400  $\mu\text{s}$  integration-time. Tests to determine the threshold for two-point resolution of echoes reveal that the limit is about 2  $\mu\text{s}$  (Simmons *et al.*, 1998).

Figures 1(c)–(f) illustrate the performance of a representative big brown bat in a jittered-echo task where the bat is rewarded for detecting the presence of changes in the arrival-time of alternating echoes (Simmons, 1993; Simmons *et al.*, 1990b). The curves show the percentage errors made by the bat as a function of the size of the time jitter between alternating echoes. In Fig. 1(c), the stimuli consist of a single electronically delivered echo for each of the bat's broadcasts, and this single echo shifts in delay back and forth from one broadcast to the next. If these jittering echoes really do differ in delay, the bat detects the jitter, performing at only a few percent errors. However, if the jitter is zero, the bat's performance is at chance ( $\sim 50\%$  errors). In Fig. 1(d), one of the two jittering stimuli consists of *two* echoes at delays separated by 10  $\mu\text{s}$ , while the other consists of only one echo. This double echo simulates two target glints and alternates with the single echo in the jitter task. The bat's performance curve in Fig. 1(d) has two peaks, one at zero and one at 10  $\mu\text{s}$ , indicating that the bat remembered both of these delay values when comparing the double and single jittering stimuli. In Fig. 1(e), the double echoes are separated by 20  $\mu\text{s}$ , and there are two error peaks separated by 20  $\mu\text{s}$ . In Fig. 1(f), the double echoes are separated by 30  $\mu\text{s}$ , and there are two error peaks separated by 30  $\mu\text{s}$ .

Because the 10–30  $\mu\text{s}$  delay separations in Figs. 1(d)–(f) are considerably shorter than the integration-time of 300–400  $\mu\text{s}$ , any information about them would have been trans-

posed from the dimension of delay itself into the peak-and-notch pattern along the frequency axis [Fig. 1(a)] during convolution of the FM sounds with the integration-time of the auditory filters. The bat's ability to recover numerical delay estimates for both echoes requires *deconvolution* to take place subsequent to formation of auditory spectrograms by the inner ear. [Figure 1(a) illustrates deconvolution by determining the correct time position for some specific horizontal slice of the plot given only the locations of the notches in frequency.] This cascade of convolution and deconvolution has been modeled as spectrogram correlation and transformation (SCAT; Saillant *et al.*, 1993). The SCAT process is the first large-scale computational model of biosonar to use a time-frequency representation extending all the way from the acoustic signals to perception, while incorporating critical aspects of auditory coding (Simmons *et al.*, 1992, 1996). It goes beyond processing of single echoes to consider the formation of delay-axis images for multiple-echo "scenes," an aspect of echolocation that has begun to receive attention (Moss and Surlykke, 2001; Simmons *et al.*, 1995). Both coherent and noncoherent versions of SCAT have been developed for evaluation against the performance of bats in experiments such as those illustrated in Figs. 1(c)–(f) (Saillant, 1995), and several important advances towards understanding echolocation have been made independently by several groups using the model (e.g., Matsuo *et al.*, 2001; Peremans and Hallam, 1998). One of these advances directly affects the experiments described here.

In the jitter performance curves there usually is a third error peak in the region of  $35 \mu\text{s}$  [arrow in Fig. 1(c)] that does not correspond to one of the nominal electronic delays. This additional peak is the focus of the work we report here. It was discovered in the first jitter experiment using analog delay lines (Simmons, 1979) and confirmed in new experiments using digital delay lines (Simmons *et al.*, 1990b). Because the time separation of the peak at zero and the additional peak at  $35 \mu\text{s}$  corresponds approximately to the spacing of the central peak and the first side-peak in the cross-correlation function of *Eptesicus* biosonar sounds with echoes (Saillant *et al.*, 1993; Simmons, 1979), it was initially taken to represent the bat's perception of this side-peak and, thus, of the crosscorrelation function itself. In effect, the additional peak at  $35 \mu\text{s}$  circumstantially appeared to represent the bat's perception of the phase of echoes relative to broadcasts. This conclusion stirred much controversy because "the mammalian" auditory system is widely assumed to be insensitive to stimulus phase for single-frequency stimuli above a few kiloHertz (Beedholm and Mohl, 1998; Menne and Hackbarth, 1986; Pollak, 1993; Schnitzler *et al.*, 1985). The controversy persisted even though the phase of wideband FM signals is analytically very different from the phase of single-frequency stimuli (Simmons, 1980). Coding of FM phase requires merely that the latency jitter of neurons registering the timing of ultrasonic frequencies in FM sweeps be smaller than the period at some frequencies, a condition satisfied in existing neurophysiological data from the auditory brainstem (Haplea *et al.*, 1994; see Casseday and Covey, 1995). To address issues raised in this controversy, less circumstantial tests for phase sensitivity were designed and incorporated

into new jitter experiments (Moss and Simmons, 1993; Simmons and Grinnell, 1988; Simmons *et al.*, 1990b), and the results demonstrated that big brown bats perceive delay with information conveyed by the phase of echoes. Once the secondary error peak at  $35 \mu\text{s}$  no longer served as the evidence for the bat's perception of echo phase, the experiments reported here were designed to identify whether there might be another source of this peak.

Interference between overlapping reflections from multiple glints is not the only way that spectral notches are introduced into echoes—the bat's external ear creates notches as echoes pass down through its structures to the eardrum. The acoustic effects of the big brown bat's external ear on sound reception (Jen and Chen, 1988; Wotton *et al.*, 1995, 1997) are much like the effects observed in humans (Asano *et al.*, 1990; Batteau, 1967; Blauert, 1983; Butler and Belendiuk, 1977; Djupesland and Zwislocki, 1973; Fisher and Freedman, 1968; Flynn and Elliott, 1965; Hebrank and Wright, 1974; Hiranaka and Yamasaki, 1983; Middlebrooks, 1992; Middlebrooks and Green, 1991; Shaw, 1982; Shaw and Teranishi, 1968; Wightman and Kistler, 1989; Wright *et al.*, 1974), in cats (Calford and Pettigrew, 1984; Musicant *et al.*, 1990; Phillips *et al.*, 1982; Rice *et al.*, 1992), in guinea pigs (Carlile and Pettigrew, 1987), and in ferrets (Carlile, 1990). In each case, the location and strength of a well-defined peak-and-notch pattern in the spectrum of sounds reaching the eardrum depends on the elevation of the sound source. The primary difference between bats and other mammals is in the *scale* of these effects—the frequencies at which the major directional effects occur are considerably higher in the big brown bat (at 25–90 kHz) than in humans (at 6–12 kHz) or cats (at 8–18 kHz), which is roughly in keeping with the size differences of the ears in these species (bats < cats < humans; see Guppy and Coles, 1988; Simmons, 1982). Figure 1(b) [inset to Fig. 1(a)] shows the approximate frequencies of notches in the directional transfer function of the big brown bat's external ear as thicker solid lines superimposed on the thinner dashed lines of Fig. 1(a) (Wotton *et al.*, 1995, 1997). Two prominent external-ear notches appear over the bat's sonar frequencies [arrow at top of Fig. 1(a)]. They shift together in frequency according to the elevation of the sound source. On average, they correspond to the placement of second- and third-order [ $n = 1$  and  $2$  in Eq. (1)] interference notches from time separations of about 15 to  $50 \mu\text{s}$  [superimposition of solid and dashed lines in Figs. 1(a) and (b)].

The measurements of external-ear notches plotted in Fig. 1(b) were made acoustically by placing a microphone at the location of the eardrum in a detached external-ear preparation (Wotton *et al.*, 1995). Behavioral measurements have also been made of the frequency of external-ear notches in echoes delivered to the bat from different elevations. Big brown bats were trained to discriminate between electronically generated echoes with a notch placed in their spectrum at a frequency of 30, 35, 40, 45, or 50 kHz and echoes without such a notch (Wotton *et al.*, 1996). These echoes were delivered to the bat from loudspeakers placed at elevations from  $-20$  to  $+20$  degrees (in 5-degree steps). When the frequency of the external-ear notch at one particular el-

DETECTION OF SPECTRAL NOTCHES  
AT DIFFERENT ELEVATIONS  
(percent errors)

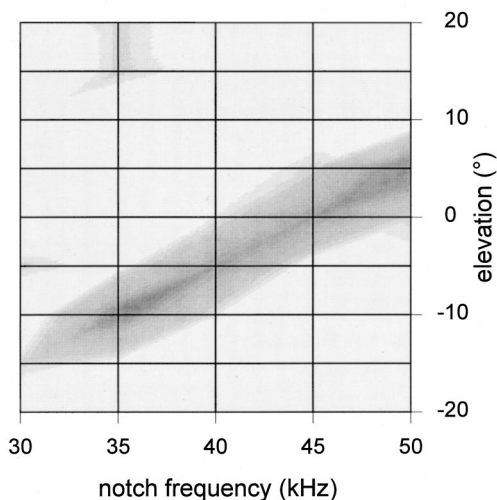


FIG. 2. Surface plot of mean percentage errors made by two big brown bats in experiments on detection of a spectral notch at 30, 35, 40, 45, or 50 kHz in artificial echoes delivered from elevations of  $-20$  to  $+20$  degrees (Wotton *et al.*, 1996). Darkest shade shows highest errors; lightest shade shows lowest errors. The sloping shaded region traces the frequencies at which masking shows that the bats perceive the external-ear notch for different elevations.

levation corresponded to the frequency of the stimulus notch introduced electronically, the bats failed to detect the echoes that had the electronic notch because the external-ear notch masked its presence. Figure 2 shows the mean performance of two bats as the percentage of errors achieved for different electronic notch frequencies and elevations (shaded from white at low errors to dark gray at high errors). The diagonal sloping band of poor performance in Fig. 2 (darkest shading) traces the perceived frequency of the external-ear notch at different elevations from its masking effect on the electronic notches. These frequencies have been transposed onto Fig. 1(b) as the five data points (open circles labeled  $+5$  to  $-15$  degrees) showing external-ear notches in the coordinates of the glint-interference plot of Fig. 1(a).

The question we address here is whether the spectral notches introduced by the bat's external ear are caught up in the deconvolution process, along with the interference notches created by the glint structure of the target, and transformed into an estimate of an extraneous time separation that ought to be dependent on the elevation of the target. The curves and data-points in Figs. 1(a) and (b) predict that this delay estimate should be somewhere in the region of 30 to 50  $\mu$ s. Does the secondary error peak at 35  $\mu$ s in Fig. 1(c) (arrow) come from notches in the frequency response of the bat's external ears? To test this hypothesis, in experiment 1 the jitter procedure was modified to allow for vertical movement of the loudspeakers that delivered the artificial echoes. If the location of the behavioral error peak at 35  $\mu$ s actually does originate in the external ear's response, this peak should move to shorter times of 25–30  $\mu$ s for loudspeaker elevations that are 15 degrees higher because the external-ear notches move to higher frequencies (Fig. 2). Conversely, this

error peak should move to longer times of 40–45  $\mu$ s for loudspeaker elevations that are 15 degrees lower because the notches move to lower frequencies. Two more experiments were done to assess the relation between external-ear notches and notches introduced into echoes by the target, prior to reception by the external ear. In experiment 1, the echoes returned electronically to the bat contained frequencies from 20 to 85 kHz, nearly the full bandwidth of the bat's FM broadcasts. In experiment 2, the echoes were filtered to a narrow region around 55 kHz, which excludes frequencies of 20–50 kHz and 60–100 kHz where external-ear notches are present. In experiment 3, the echoes were filtered to a different narrow frequency band around 45 kHz, which preserves frequencies of 40–50 kHz where the external-ear notches *do* occur.

## II. METHOD

The experiments described here were carried out using three bats of the species *Eptesicus fuscus* (see Kurta and Baker, 1990), collected in houses in the State of Rhode Island and Providence Plantations (identified as bats 3, 5, and 6 in Simmons *et al.*, 1990b). The bats were trained in a two-choice discrimination task (2AFC; see Moss and Schnitzler, 1995) to distinguish between sonar echoes that *jittered* or *alternated* in delay and echoes that were *stationary* in delay. Stimulus echoes were produced by an electronic target simulator incorporated into the two-choice behavioral procedure. Figure 3 shows the psychophysical paradigm for jittering-echo experiments (Simmons *et al.*, 1990b). Each bat was trained to sit on an elevated, Y-shaped platform and broadcast echolocation sounds towards the left and right to find an electronically simulated target that appeared to alternate in target range from one sonar emission to the next. This jittering target (represented by echoes *a* and *b* in Fig. 3) was presented either on the bat's left or the bat's right in the two-choice task, with the stationary target (*c*) presented on the other side. The bat was rewarded with a piece of a mealworm offered in forceps for every correct response, which was to move forward towards to the jittering target (arrow). Responses to the stationary (nonjittering) stimulus were not rewarded, and a brief time-out period was introduced before proceeding to the next trial.

The target simulator is described in detail elsewhere, together with various procedures developed to calibrate it and eliminate stimulus artifacts that might interfere with the bat's use of echo delay as the chief cue for the discrimination (Simmons, 1993; Simmons *et al.*, 1990b). These sources also describe the use of amplitude-latency trading to demonstrate that the curve in Fig. 1(c) represents perceived values of delay that depend on the latencies of neural responses rather than spurious performance not involving perception of delay itself (Beedholm and Mohl, 1998; Menne *et al.*, 1989; Polak, 1993; Schnitzler *et al.*, 1985). The experiments reported here involve only the use of digital electronic delays.

The jittering echoes (*a* alternating with *b* in Fig. 3) and stationary echoes (*c* alternating with *c*) were simulated electronically by picking up the bat's sonar transmissions with two Brüel & Kjaer Model 4138 condenser microphones (*m* in Fig. 3), amplifying and filtering the signals with Rockland

## BEHAVIORAL TASK

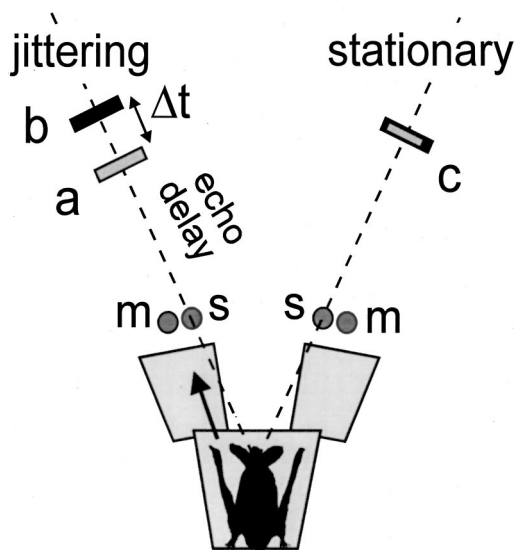


FIG. 3. Diagram of the jittered-echo procedure and the two-choice psychophysical method for determining the shape of the bat's echo-delay images in terms of the delays the images are perceived to contain (Simmons *et al.*, 1990b). The bat sits on the Y-shaped platform, broadcasts sonar sounds into microphones (*m*), whose output signals are delayed and then returned to the bat as simulated echoes from one of the two loudspeakers (*s*) according to which microphone the bat aims its sounds towards. If delivered from the jittering channel, the delays of successive echoes alternate between two values (*a*, *b*); if from the stationary channel, the delays are fixed (*c*).

Model 442 variable bandpass filters normally set to a pass-band from 15 to 100 kHz, and then returning these recorded sounds back to the bat from two RCA Type 112343 electrostatic loudspeakers (*s*). The echoes produced by this means were timed to arrive at appropriate delays following the bat's transmissions to mimic echoes from a target at a specific distance. The microphones (*m*) and loudspeakers (*s*) were about 20 cm from the bat's observing position on the Y-shaped platform, so the acoustic travel time from the bat to the microphones and then back from the loudspeakers was about 1.16 ms. The total delay of echoes was regulated by adding an electronic delay to this propagation delay, assuming that each centimeter of simulated target range would require 58  $\mu\text{s}$  more delay. In the experiments, the overall delay of echoes from the simulated stationary target (*c*) was fixed 3.275 ms, which corresponds to a distance of about 56 cm. The jittering echoes (*a* and *b*) were presented at delays that were centered on 3.275 ms but were shifted by  $\pm$  half the jitter interval ( $\pm \Delta t/2$ ) around that value (Simmons *et al.*, 1990b). The stimuli are described later in terms of the size of the jitter interval because this is the principal independent variable being manipulated, but the absolute echo delays used to achieve different amounts of jitter always were arranged around 3.275 ms.

The delay of stimulus echoes was adjusted electronically using digital delay devices (*delay* in Fig. 3) that sampled the bat's signals at 730 kHz (12-bit accuracy) and then stored them for a preset time in a buffer memory before playing them back through a digital-to-analog converter. Because the

numerical value of delay depends only on digital control of the address of the word being read out from the memory through the D-to-A converter, no delay-dependent changes in the spectrum of echoes were introduced by the digital delay lines, so no apparatus-related artifacts are suspected (see Beedholm and Mohl, 1998). The left and right channels of the simulator each contained two digital programmable delay lines for presenting echoes at any desired times from 0 to about 41 ms following emissions, and associated electronic components were used to switch one or another of these delay-lines on for each of the bat's broadcasts (Simmons *et al.*, 1990b). The critical feature of these jittered-echo experiments is that this switching system delivered only *one electronic echo to the bat for each sonar broadcast*. Depending on whether the left or right microphone received the stronger signal for any of the bat's broadcasts, only the corresponding left or right delay system and loudspeaker was activated to deliver an echo. Successive broadcasts yielded echoes only from the channel the bat aimed its sounds towards. This contingency requires the bat to remember the delay of one echo for comparison with the delay of the next to detect whether jitter is present. The jittering stimulus was created by setting the delays of the echoes for successive broadcasts (*a*, *b*) so that they alternated back and forth over the jitter interval ( $\Delta t$ ). The stationary stimulus (*c*) was created by setting the delays so that successive echoes always had the same delay. Both the stationary and the jittering stimuli were generated by alternately switching the bat's broadcasts between delay values created by two different delay-lines; whether the stimuli jittered depended only the values of delay actually selected digitally, not on whether the signal passed through any one piece of hardware.

The frequency response for the left and right channels of the target simulator was limited by the loudspeakers to a range from 20 kHz to about 85 kHz (Simmons *et al.*, 1990b), but it could be further restricted to a narrower range by resetting the bandpass filters to any desired high- and lowpass cut-off frequencies. The highest frequency present in the sounds reaching the bat's ears was about 85 kHz, for a Nyquist sampling frequency of 170 kHz. The actual digital sampling frequency of the apparatus was about 730 kHz, which is much higher than the Nyquist frequency to be sure that the time-series sound-pressure waveform of simulated sonar echoes would be faithfully reproduced in the analog signals delivered to the loudspeakers. (Whereas sampling at the Nyquist frequency is the minimum adequate to determine the bat signal's spectrum, sampling at rates several times the Nyquist frequency is necessary to reproduce its cycle-by-cycle waveform.)

At the beginning of the jitter experiment, the jitter interval ( $\Delta t$ ) was set to a value in the range of 50 to 70  $\mu\text{s}$ , which is easy for bats to detect—they normally achieve about 90%–95% correct responses (Simmons, 1979; Simmons *et al.*, 1990b). The size of this interval then was reduced gradually from 50–70  $\mu\text{s}$  to 0  $\mu\text{s}$  in steps of approximately 5  $\mu\text{s}$ . On two occasions, a smaller delay step-size of 2.5  $\mu\text{s}$  was used to interpose a data-point between two 5- $\mu\text{s}$  points because the performance of the bat suggested that a smaller interval would better capture an intervening peak in perfor-

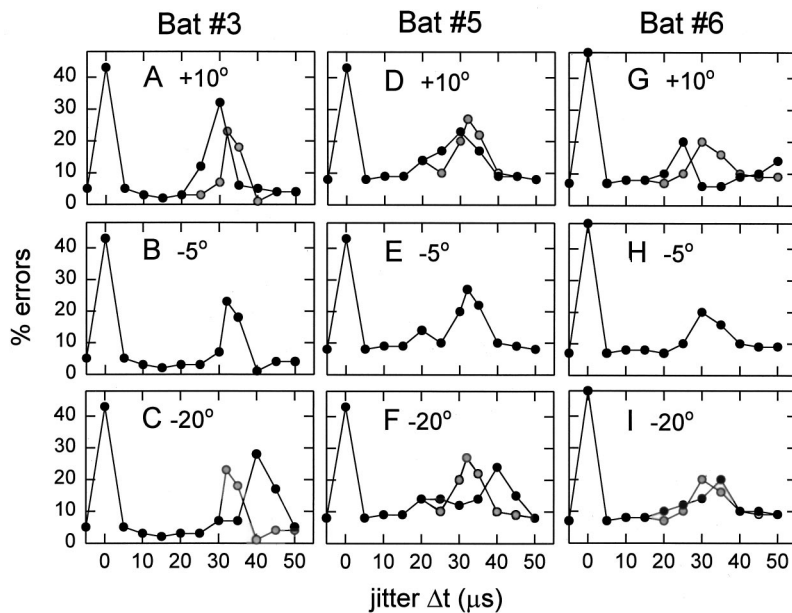


FIG. 4. Results of experiment 1: Graphs showing the jittering-echo discrimination performance (percentage errors; black lines, black circles) of three big brown bats (bats 3, 5, and 6) with loudspeakers at elevations of +10, -5, and -20 degrees. The curves from the middle plots (b, e, h) showing performance at -5 degrees are repeated (gray lines, gray circles) in the upper (a, d, g) and lower (c, f, i) plots to facilitate comparisons. The bats all perform near chance (50%) when the jittering echoes have the same delay,  $\Delta t = 0 \mu s$ , and they also all have a secondary region of poor performance at  $\Delta t = 25$  to  $45 \mu s$ . For all three bats the location of this secondary peak depends on the elevation of the loudspeakers.

mance that was straddled by the  $5\text{-}\mu s$  interval. The  $5\text{-}\mu s$  step size was the largest interval used because it is shorter than the Nyquist sampling interval for the stimuli. The data from the jitter discrimination experiments consist of the mean performance of each bat on 40 to 60 trials conducted at each jitter interval before moving to the next smaller interval in the series. To display the results, the percentage of correct responses or errors for each bat was graphed as a function of the size of the jitter interval ( $\Delta t$ ) from  $50\text{--}70 \mu s$  down to  $0 \mu s$  in steps of  $5 \mu s$ . During the course of this decreasing series of jitter intervals, the bat's performance eventually reaches chance, about 50% correct responses, when the jitter interval is zero. However, the level of performance does not decline monotonically to chance; instead it passes through a region of poor performance around  $35 \mu s$  [arrow in Fig. 1(c)] and then recovers again for jitter intervals from  $25 \mu s$  down to very near  $0 \mu s$ .

To assess the possible role of the external ear in causing the bat to make errors at certain jitter intervals, the positions of the loudspeakers on the bat's left and right ( $s$  in Fig. 3) were changed by  $\pm 15$  degrees in elevation relative to the bat. The Y-shaped platform used for two-choice tests was tilted downward at an angle of  $15\text{--}20$  degrees to accommodate the bat's inclined stance on its thumbs and feet with the wings folded. While the bat stood on the platform for its response on each trial, its head and body were not parallel to the plane of the platform but were held at an angle about 10 degrees higher, as estimated from photographs, which left the eye-nostril plane of the bat's head still tilted about 5 degrees below the horizontal. The loudspeakers used in the basic jitter experiments (Simmons *et al.*, 1990b) protruded 10 degrees above the plane of the platform, and the bat's posture and movements kept the eye-nostril plane about 5 degrees above the loudspeakers, which placed the microphones roughly in line with the bat's open mouth. The normal position of the loudspeakers thus was at an elevation of about  $-5$  degrees relative to the bat's head.

### III. EXPERIMENT 1

#### A. Hypothesis

Experiment 1 explicitly tested the possibility that the region of poor performance around  $35 \mu s$  in Fig. 1(c) (arrow) is elevation dependent by repeated the basic jitter experiment for jitter values in this region ( $20\text{--}50 \mu s$  depending on the bat) using different elevations of the loudspeakers ( $s$ ). The essential experimental manipulation was to change the position of these loudspeakers by moving them either 15 degrees higher or 15 degrees lower than normal. The three loudspeaker positions were designated by their elevations as +10, -5, and -20 degrees relative to the bat's eye-nostril plane. It is unlikely that serial order effects are present because the three bats were run at different times interspersed among different jitter experiments that measured acuity in the submicrosecond range, performance for echo phase shifts, or acuity as a function of changes in echo bandwidth controlled by the bandpass filters in the microphone circuit (Simmons *et al.*, 1990b).

#### B. Results

Three *Eptesicus* (3, 5, and 6) completed experiment 1 with the loudspeakers moved upward or downward by 15 degrees from their normal position at  $-5$  degrees relative to the bat's head in its posture on the platform. Figure 4 shows the results for each bat at each elevation of the loudspeakers. The middle row of graphs [Figs. 5(b), (e), and (h); black lines, black circles] shows the basic jitter discrimination performance for each of these bats at loudspeaker positions of  $-5$  degrees elevation (see Simmons *et al.*, 1990b). The curve for each bat shows errors in the range of only 5%–10% for jitter intervals ( $\Delta t$ ) from  $50 \mu s$  down to  $40 \mu s$  (performance was also this good for jitter intervals  $> 50 \mu s$ ), with a region of poorer performance of 20%–30% errors at 30 to  $35 \mu s$ , and good performance again at jitter intervals from  $25 \mu s$  down to only  $5 \mu s$ . At  $0 \mu s$ , performance was

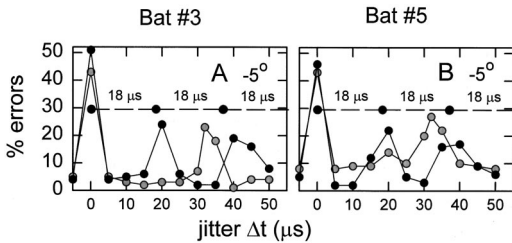


FIG. 5. Results of experiment 2: Graphs (a, b) showing the jittering-echo discrimination performance (percentage errors; black lines, black circles) of two big brown bats (bats 3 and 5) with loudspeakers at an elevation of  $-5$  degrees and echoes restricted to around 55 kHz. The bat's performance at  $-5$ -degree elevation with the full bandwidth of echoes [gray lines, gray circles, from Figs. 4(b) and (e)] is shown to facilitate comparisons. Both bats shift the pattern of error peaks from 0 and 30–35  $\mu$ s (gray) to 0, 20, and 35–40  $\mu$ s (black).

always near chance, or 50%, thus forming the primary peak in the error curve. Each bat also exhibited a second, lower peak in the error curve at 30–35  $\mu$ s when the loudspeaker was at an elevation of  $-5$  degrees relative to its head.

The *top* row of graphs [Figs. 4(a), (d), and (g); black lines, black circles] shows the change in performance of these same three bats in the region of the secondary error peak when the loudspeakers were moved up to an elevation of  $+10$  degrees. (For each bat, the gray lines with gray circles repeat the data from  $-5$  degrees elevation to facilitate comparison of results by eye.) There is a shift in the location of the secondary region of poor performance to shorter time values, from 30–35  $\mu$ s to 25–30  $\mu$ s. The *bottom* row of graphs [Figs. 4(c), (f), and (i); black lines, black circles] shows the performance of the bats when the loudspeakers were moved down to an elevation of  $-20$  degrees. (Again, the gray lines with gray circles repeat the data from  $-5$  degrees elevation.) Here there is a shift in the location of the secondary region of poor performance to longer time values, from 30–35  $\mu$ s to 35–45  $\mu$ s. For all three bats, the secondary error peak in the performance curve marked by the arrow in Fig. 1(c) shifted to shorter time values for the higher loudspeaker elevation and longer time values for the lower elevation. Pooling data from all three bats, the exchange of the peak in the error curves between locations over a span of 5  $\mu$ s from  $-5$  to  $+10$  degrees and again from  $-5$  to  $-20$  degrees is statistically significant using the binominal distribution for 2AFC data.

### C. Discussion

For each bat, the location of the secondary error peak in Fig. 4 depends systematically on the vertical position of the loudspeakers. In each case, the peak was shifted by about 5  $\mu$ s in the direction predicted from the external-ear transfer function (Fig. 2). The higher external-ear notch frequency associated with higher elevations (Fig. 1) leads to a shorter time value, while the lower notch frequency at lower elevations leads to a longer time value. Moreover, the locations of the error peaks along the time axis in Fig. 4 are approximately where they would be expected from reading the time values associated with the five data-points on the interference-notch graph in Figs. 1(a) and (b). Depending on

elevation, the expected range of time values is roughly 30–50  $\mu$ s from the vertical axis of Fig. 1(a), while the error peaks actually are located at values of 25–45  $\mu$ s. To a first approximation, big brown bats appear to treat the notch in the external-ear transfer function at frequencies of 30–50 kHz as though it were a second-order interference notch in the echoes [ $n=1$  in Eq. (1)], and they engage this notch in their deconvolution process (Saillant *et al.*, 1993; Simmons *et al.*, 1996) when they transform the time-frequency structure of echoes into remembered delays.

## IV. EXPERIMENT 2

### A. Hypothesis

The echoes used as stimuli in experiment 1 had almost the full bandwidth of the bat's FM biosonar sounds, limited only by the frequency response of the loudspeakers in the highest-frequency region (see Simmons *et al.*, 1990b). Echo frequencies extended from 20 kHz to about 85 kHz, which includes the frequencies of spectral notches produced by the external ear [Fig. 1(b)]. What happens to the bat's performance when the frequency range of the external-ear notches is deliberately removed from echoes prior to reception? In experiment 2, electronic echoes were restricted to the region of 55 kHz using the Rockland Model 442 variable bandpass filters already part of the microphone circuit. All echoes (*a*, *b*, and *c* in Fig. 3) were filtered identically and then increased in overall amplitude by 2 dB to compensate for the measured loss in signal strength at the 55-kHz center frequency of the passband due to the filters' characteristics. The narrow passband thus affected the jittering and stationary echoes alike. The filters gave 24-dB/oct rolloffs to yield 3-dB lowpass and highpass cutoffs at frequencies of about 50 and 60 kHz, respectively. Using these filter settings, the jitter experiment was carried out with the loudspeakers at the normal elevation of  $-5$  degrees. This 55-kHz band is special because it excludes the frequency region around 40–45 kHz where the bat's most prominent external-ear notch occurs at a loudspeaker elevation of  $-5$  degrees (see Fig. 2). In the absence of a recognizable external-ear notch at 40–45 kHz and also at frequencies above 60 kHz (because this notch region is obliterated from 55-kHz echoes, too), we hypothesized that the bat should perceive only those delay separations that satisfy the impulse response for band-limited echoes at 55 kHz. The jitter performance curve should contain multiple error peaks at a nominal spacing of approximately  $1/55 \text{ kHz} = 18 \mu\text{s}$ . In other respects, experiment 2 was conducted exactly as was experiment 1.

### B. Results

Two of the bats (bats 3 and 5) went through experiment 2 with the loudspeakers at the normal elevation of  $-5$  degrees. Figures 5(a) and (b) show both bats' performance in the 55-kHz band-limited condition (black lines, black circles) compared to performance with practically the full bandwidth of the bat's sounds [gray lines, gray circles; taken from Figs. 4(b) and (e), respectively]. [Data for bat 3 were given in Fig. 11 of Simmons *et al.* (1990b).] Consistently for both bats, the shape of the performance curve for

narrow-band 55-kHz echoes is different from that obtained in the same task with broadband echoes. In Fig. 5, instead of a main error peak at 0  $\mu\text{s}$  and a single secondary error peak at 30–35 (gray), there is a main peak at 0  $\mu\text{s}$  and secondary peaks located at 20  $\mu\text{s}$  and 35–45  $\mu\text{s}$  (black). Each peak is well defined, being surrounded by a low error rate on its flanks. These error peaks represent statistically significant departures from the low error rates prevailing at intermediate delays using the binomial distribution.

### C. Discussion

When the bandwidth of echoes is restricted to 50–60 kHz, they simulate a periodic impulse response with a series of peaks at times of 0, 18, 36, 54, ...  $\mu\text{s}$ . The locations of these theoretical peaks are indicated in Figs. 5(a) and (b) by the horizontal dashed lines (with black circles at 18- $\mu\text{s}$  separations). In these same plots, the jitter performance curves for the two bats in experiment 2 have multiple error peaks at 0, 20, and 35–40  $\mu\text{s}$ . The bats' performance thus corresponds approximately to the simulated target impulse response. The elevation-dependent error peak, formerly located at about 35  $\mu\text{s}$  for an elevation of  $-5$  degrees, is no longer present, presumably because the external-ear notches that signify interference at a delay separation of 35  $\mu\text{s}$  are no longer recognizable in the echoes due to the wholesale absence of frequencies below 50 kHz and above 60 kHz.

## V. EXPERIMENT 3

### A. Hypothesis

The echoes in experiment 2 were restricted to the region of 55 kHz to exclude frequencies from 20 to 50 kHz and from 60 to 100 kHz, thereby preventing echoes from containing the frequency regions most important for conveying external-ear notches. The echoes used in Experiment 3 were band-limited, too, but this time to a frequency of 40 kHz. In this case the Rockland filters gave 24-dB/octave rolloffs with 3-dB lowpass and highpass cutoff points at about 35 and 45 kHz, respectively. This passband gave continuous coverage of frequencies where the bat's most prominent external-ear notch occurs at loudspeaker elevations of  $0^\circ$  to  $-10^\circ$  (Fig. 2), and appreciable coverage was present over a somewhat wider band of frequencies occupied by the notch at elevations from at least  $+5^\circ$  to  $-15^\circ$ . Again, in experiment 3, all echoes (*a*, *b*, and *c* in Fig. 3) were filtered identically and then increased in overall amplitude by 2 dB to compensate for the measured loss in signal strength at the 40-kHz center frequency. The target impulse response simulated by these echoes has an average period of  $1/40 \text{ kHz} = 25 \mu\text{s}$ , with a main peak at 0  $\mu\text{s}$  followed by a series of side peaks at 0, 25, 50, 75, ...  $\mu\text{s}$ .

Figure 6 illustrates our hypothesis of what would be expected in experiment 3 from using the 40-kHz narrow-band echoes in the jitter experiment. If the bat's performance curve is determined by the target impulse response, we would expect to see a series of error peaks at 0, 25, and 50  $\mu\text{s}$  on the horizontal axis of Fig. 7 (horizontal dashed line with three black circles separated by 25- $\mu\text{s}$  intervals at the top of the graph). The black curve in Fig. 6 shows the ap-

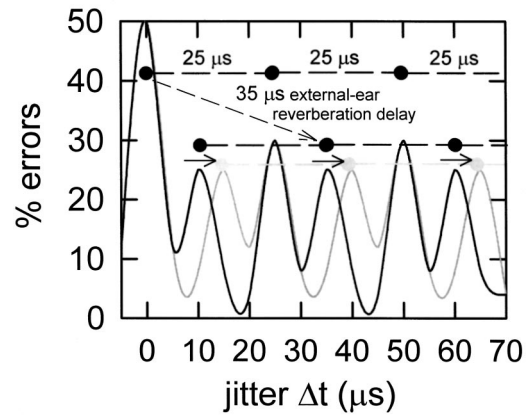


FIG. 6. Graph showing the jitter discrimination performance (percentage errors) expected to occur if the simulated echoes are filtered to a narrow band around 40 kHz (3-dB points at 35 and 45 kHz) for loudspeaker elevations of  $-5$  degrees (black curve) and  $-20$  degrees (gray curve). The basis for this prediction is that the simulated target impulse response contains a series of peaks separated by 25  $\mu\text{s}$  (horizontal dashed line with black circles at top of plot) plus an added series of peaks shifted to the right by the external-ear reverberation delay of 35  $\mu\text{s}$ , and still separated by 25  $\mu\text{s}$  (horizontal dashed line with black circles at middle of plot). Experiment 3 tests whether the bat's performance contains this configuration of peaks, and whether the peaks corresponding to the external-ear reverberation change with loudspeaker elevation (black curve *versus* gray curve).

proximate percentage errors that a bat should achieve in experiment 3. Besides the three error peaks at 0, 25, and 50  $\mu\text{s}$ , this solid curve has three additional error peaks representing the delays derived from spectral notches introduced by the external ear. At the normal loudspeaker elevation of  $-5$  degrees, the expected external-ear delay should be 30–35  $\mu\text{s}$ , based on the single secondary error peak at 30 to 35  $\mu\text{s}$  in Figs. 4(b), (e), and (h). In experiment 3, this single secondary peak should be replaced by a series of secondary peaks separated by 25- $\mu\text{s}$  intervals and offset to the right of zero by 30–35  $\mu\text{s}$  (horizontal dashed line with three black circles at the middle of Fig. 6). These additional peaks should shadow the main peaks and appear to follow them 10  $\mu\text{s}$  later, at 10, 25, and 60  $\mu\text{s}$  on the time axis of Fig. 6. (The real offset of the external-ear peaks is 35  $\mu\text{s}$ , but each external-ear peak winds up only 10  $\mu\text{s}$  later than the nearest peak from the simulated target's impulse response.) Knowing that 55-kHz echoes leads to error peaks at 0, 20, and 35–40  $\mu\text{s}$  in experiment 2, the prediction of three error peaks at 0, 25, and 50  $\mu\text{s}$  in experiment 3 should come as no surprise. However, the bat's external ear contributes three additional predicted error peaks at 10, 35, and 60  $\mu\text{s}$ , which is a more complicated result. If these additional peaks do occur in experiment 3 for a loudspeaker elevation of  $-5$  degrees (black curve in Fig. 6), then a test of whether they originate in external-ear notches would be to repeat the 40-kHz experiment at a different loudspeaker elevation, just as was done in experiment 1 for broadband echoes. The gray curve in Fig. 6 shows expected results for the 40-kHz echoes with the loudspeaker at an elevation of  $-20$  degrees instead of  $-5$  degrees. The target-related error peaks in the  $-5$  degrees hypothetical performance curve at 0, 25, and 50  $\mu\text{s}$  (black curve) should remain in the same locations for an elevation of  $-20$  degrees (gray curve), but the external-ear peaks at

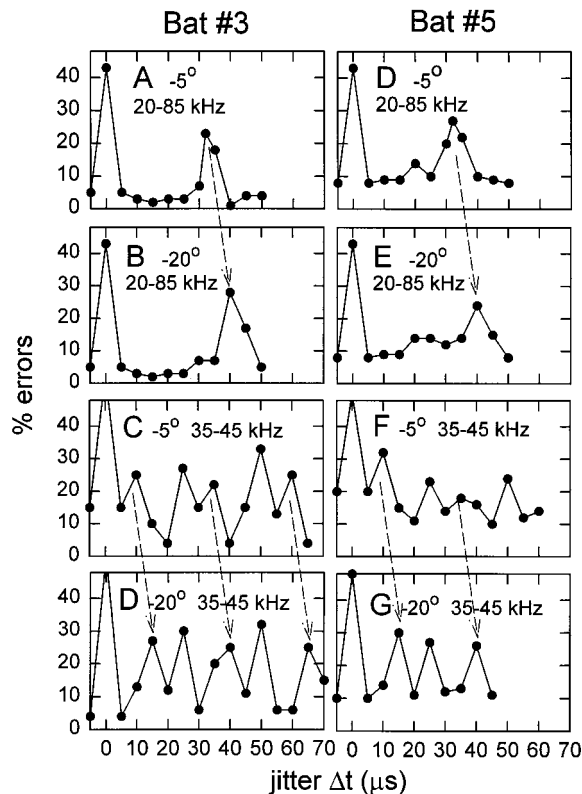


FIG. 7. Results of experiment 3: Graphs showing the jittering-echo discrimination performance (percentage errors; black lines, black circles) of two big brown bats (bats 3 and 5) with loudspeakers at elevations of  $-5$  and  $-20$  degrees and echoes restricted to around 40 kHz. The top two rows of plots (a, b and d, e) show performance for the full bandwidth of echoes (20–85 kHz) from experiment 1 [Figs. 4(b), (c), (e), and (f)] for comparison. The bottom two rows of plots (c, d, f, g) show performance for the narrow-band echoes (35–45 kHz) in experiment 3. The bats perform near chance (50%) when the jittering echoes (a, b) have the same delay,  $\Delta t = 0 \mu\text{s}$ , and, when the loudspeakers are at  $-5$  degrees (c, f), they also have multiple secondary peaks of poor performance at  $\Delta t = 10, 25, 35, 50,$  and  $60 \mu\text{s}$ . When the loudspeakers are at  $-20$  degrees (d, g), the bats also have multiple secondary peaks of poor performance at  $\Delta t = 15, 25, 40, 50,$  and  $65 \mu\text{s}$ . The series of peaks at 0, 25, and  $50 \mu\text{s}$  do not shift with loudspeaker elevation, while the series of peaks at 10, 35, and  $60 \mu\text{s}$  shift to the right by  $5 \mu\text{s}$  (sloping arrows in c, d and f, g) when the loudspeakers are moved  $15^\circ$  down. The single secondary error peak in experiment 1 also shifts by  $5 \mu\text{s}$  (sloping arrow in a, b and d, e) when the loudspeakers are moved  $15$  degrees down.

10, 35, and  $60 \mu\text{s}$  should move to the right by about  $5 \mu\text{s}$  to locations of 15, 40, and  $65 \mu\text{s}$  (gray curve; see short horizontal arrows in Fig. 6). This outcome is what would be expected if the external-ear delay increased from 35 to  $40 \mu\text{s}$ , as it did in experiment 1. Experiment 3 was carried out with loudspeaker elevations of  $-5$  and  $-20$  degrees using echoes filtered to the 35–45-kHz frequency band and jitter intervals from 0 to 45–70  $\mu\text{s}$ . In other respects, experiment 3 was conducted exactly as was experiment 1.

## B. Results

Two of the bats (bats 3 and 5) completed experiment 3. One bat (bat 3) finished all trials at  $-5$ - and  $-20$ -degree loudspeaker elevations, while the other bat (bat 5) finished all trials at the  $-5$ -degree elevation and trials from 0 to 45  $\mu\text{s}$  at the elevation of  $-20$  degrees. Figure 7 shows the per-

formance of bats 3 and 5 in experiment 3 at loudspeaker elevations of  $-5$  degrees [Figs. 7(c) and (f)] and  $-20$  degrees [Figs. 7(d) and (g)], for comparison with data from experiment 1 [Figs. 7(a, d) and (b, e)]. Consistently for both bats, the shape of the performance curve for 40-kHz narrow-band echoes at  $-5$  degrees is different from the curve obtained in the same task with broadband echoes, and different, too, than the curve obtained for echoes band-limited to 55 kHz. Instead of a main error peak at  $0 \mu\text{s}$  and a single secondary error peak at 30–35  $\mu\text{s}$  (for the broadband echoes at an elevation of  $-5$  degrees), there are multiple peaks located at 0, 10, 25, 35, 50, and  $60 \mu\text{s}$  [Figs. 7(c) and (f)]. These peaks represent statistically significant departures from the low level of errors expected at locations away from  $0 \mu\text{s}$  using the binomial distribution.

## C. Discussion

When the bandwidth of echoes is restricted to 35–45 kHz, they simulate a periodic target impulse response with a series of peaks at times of 0, 25, 50, ...  $\mu\text{s}$ . The locations of these theoretical peaks are indicated in Fig. 6 by the upper horizontal dashed line with black circles at 25- $\mu\text{s}$  separations. Preserving the frequencies of the most prominent external-ear notch in these narrow-band echoes should lead to a complex impulse response for the stimuli at the bat's eardrum with additional peaks offset from the target's peaks by 35  $\mu\text{s}$ . Their locations are indicated in Fig. 6 by the lower horizontal dashed line with black circles for external-ear reverberation delay. Comparing Figs. 7(a) and (d) with Figs. 7(c) and (f), the bats' performance curves for a loudspeaker elevation of  $-5$  degrees change from one primary error peak at  $0 \mu\text{s}$  plus a secondary peak at 30–35  $\mu\text{s}$  for broadband echoes to a complex pattern of multiple error peaks at 0, 10, 25, 35, 50, and  $60 \mu\text{s}$  for 40-kHz narrow-band echoes. This arrangement of peaks is consistent with the prediction (black curve in Fig. 6) that both the simulated target impulse response and the external-ear reverberation time should contribute to the shape of the jitter performance curve. Moreover, when the loudspeakers were moved from  $-5$  degrees to an elevation of  $-20$  degrees, the error peaks at 0, 25, and  $50 \mu\text{s}$  remained in place [Figs. 7(d) and (g)] while the error peaks at 10, 40, and  $60 \mu\text{s}$  each shifted to the right by about  $5 \mu\text{s}$  to 15, 40, and  $65 \mu\text{s}$  [following the sloping dashed arrows in Figs. 7(d) and (g)]. This new arrangement of peaks also is consistent with the prediction (black and gray curves in Fig. 6) that both the simulated target impulse response and the elevation-dependent external-ear reverberation time contribute to the shape of the jitter performance curve. Note that the movement of the three putative secondary external-ear error peaks in experiment 3 is the same as the movement of the single putative secondary external-ear error peak in experiment 1 (compare sloping arrows connecting the different plots in Fig. 7).

## VI. CONCLUSIONS

The primary outcome of experiments 1–3 concerns the nature of the biosonar images perceived by big brown bats. Taken together, the results demonstrate that the notches in

the directional transfer function for the big brown bat's external ear are treated the same way as interference notches introduced into echoes by multiple reflections from the target. They are caught up in the SCAT deconvolution process that underlies wideband biosonar imaging and converted into numerical estimates for time separations. The bat's perception of delay estimates derived from the external ear's acoustic properties as well as from the target's glints confirms that the big brown bat's images correspond approximately to the impulse response of the target-range scene constructed from echoes reaching the eardrum (Simmons *et al.*, 1992; Simmons, 1989, 1996). Given the limitation on purely time-domain representation from the long integration-time of echo reception, we conclude that this impulse response arises from time-frequency SCAT computations carried out by the auditory nervous system (Saillant *et al.*, 1993; Sanderson and Simmons, 2000, 2002; Simmons *et al.*, 1996). Inasmuch as the perceived delays are manifested as error peaks in the performance curves from jittered-echo experiments, these curves are themselves plots of the impulse response of the stimuli, obtained by using the bat as a time-frequency processor.

The appearance of error peaks at approximately the predicted, elevation-dependent delay values of 25–50  $\mu$ s in experiment 1 shows that perceived values of delay derived from the external-ear response can be expected to occur for bats echolocating in natural conditions, where they receive essentially the full bandwidth of echoes from targets at distances up to several meters. The failure of additional error peaks (besides those related to the target) to occur in experiment 2 with narrow-band echoes shows that their manifestation is tied to reception of frequencies containing external-ear notches. The reappearance of the elevation-dependent error peaks in experiment 3 shows that the narrow-band condition itself is not the reason for the disappearance of the peaks in experiment 2. Instead, their disappearance is due to removal of frequencies containing external-ear notches. The complicated result obtained in experiment 3 shows that each of the target-related delay estimates, derived from the timing and interference of replicas of the broadcast impinging on the external ears, comes to be associated with corresponding delay estimates that depend on the elevation of the target.

Because spectral notches in echoes have more than one source, they are ambiguous indicators of the acoustic environment to the bat. Echolocating big brown bats certainly are exposed to masking between elevation and perceived spectral features—they cannot detect a notch at a particular frequency in the spectrum of echoes if the sounds arrive from an elevation where the external-ear transfer function places its own notch at the same frequency (Wotton *et al.*, 1996; see Fig. 2). Convergence of both the target's glints and the external ears on the echo spectrum creates uncertainty about whether any particular spectral notch signifies information about the target's shape or about its elevation. However, during aerial pursuits FM bats do not exhibit any obvious deficits in the accuracy of vertical localization of airborne targets related to their shape (although careful observations might disclose them). Moreover, FM bats maneuver successfully through complex obstacle arrays (Schnitzler and Henson,

1980; Simmons *et al.*, 1995) or perform unexpectedly difficult tasks in nature (Simmons *et al.*, 2001) where there is great scope for multiple reflections to interfere with each other while simultaneously the external ears introduce notches into echoes according to elevation, so they might have developed methods for resolving ambiguous spectral cues, presumably by exploiting characteristics of their auditory representation of FM broadcasts and echoes.

The SCAT model of auditory processing in FM biosonar is a hybrid computational system that creates parallel/convergent time-domain and frequency-domain representations (Saillant, 1995; Saillant *et al.*, 1993). SCAT's parallel time and frequency representations offer computational advantages if information can be passed back and forth between the two domains during processing (Simmons *et al.*, 1992). The logic is that the time-domain (impulse response) and frequency-domain (spectral) representations are both multi-valued functions, but in certain instances each can be transformed into a single value of the other. For example, a series of spectral notches, which requires a whole sequence of frequency-amplitude coefficients for its description, often can be represented by a single time separation, assuming that the notches are created by interference [Fig. 1(a)]. In the course of a recent investigation aimed at improving the SCAT model, the potential ambiguity between interference notches and external-ear notches was directly addressed by exploiting back-and-forth convergences in the dual SCAT architecture to mitigate crosstalk between the target's glints and its elevation, at least for targets having a simple glint structure (Matsuo *et al.*, 2001). One way to resolve this ambiguity would be to block out a specific region of frequencies in echoes to be reserved for registering the elevation of targets from external-ear notch cues by ignoring notches at these frequencies as far as target reconstruction is concerned. Target impulse responses derived from SCAT would be incomplete due to the deliberate exclusion of notches at these "forbidden" frequencies, but there would be reduced confusion between target shape and elevation. This recent study achieved an ingenious solution by exchanging information between the time- and frequency-domains in several stages (see especially Fig. 5 in Matsuo *et al.*, 2001)—(1) blocking out echo frequencies associated with the most prominent external-ear notch (see Fig. 2), (2) estimating the target impulse response from the pattern of notches in the remainder of the echo spectrum, (3) sharpening the peak of this incomplete impulse response and transforming it back into the frequency domain to estimate only the target's contribution to the spectrum, including the forbidden frequencies, (4) transforming this purified target-related spectrum back into the time domain, and (5) subtracting the purified target impulse response from the more complex impulse response obtained from the original echo spectrum before blocking, which includes both the target and the external ear's effects, to leave a residue that isolates the external ear's effects. Otherwise, the most conservative conclusion is that the results obtained in experiments 1–3 just shift the locus of target versus external-ear ambiguity from the frequency domain, where common practice finds it convenient to describe the stimuli, to the time domain, where the results show that *Eptesicus*

may actually perceive the ambiguity to exist. The broader conclusion is that the characteristics of the external-ear response may be *incorporated into perception of target range itself* by becoming attached to the object as a sort of ghost glint at an elevation-dependent time separation. To the bat, sonar targets thus may be perceived as having glints at specific delays for the purpose of determining their elevation, which is a different proposition than just that elevation is determined from the frequencies of notches in the external-ear transfer function.

## ACKNOWLEDGMENTS

This research was supported by NIDCD Grant No. DC-00511, by ONR Grant No. N00014-89-J-3055, by NIMH Research Scientist Development Award MH-00521, and by a grant from the Deafness Research Foundation. We thank numerous colleagues who have provided advice or assistance in the conduct of this research.

Altes, R. A. (1984). "Texture analysis with spectrograms," *IEEE Trans. Sonics Ultrason.* **SU-31**, 407–417.

Asano, F., Suzuki, Y., and Sone, T. (1990). "Role of spectral cues in median plane localization," *J. Acoust. Soc. Am.* **88**, 159–168.

Batteau, D. W. (1967). "The role of the pinna in human localization," *Proc. R. Soc. London, Ser. B* **168**, 158–180.

Beedholm, K., and Mohl, B. (1998). "Bat sonar: An alternative interpretation of the 10-ns jitter result," *J. Comp. Physiol., A* **182**, 259–266.

Beuter, K. J. (1980). "A new concept of echo evaluation in the auditory system of bats," in *Animal Sonar Systems*, edited by R.-G. Busnel and J. F. Fish (Plenum, New York), pp. 747–761.

Blauert, J. (1983). *Spatial Hearing: The Psychophysics of Human Sound Localization* (MIT, Cambridge, MA).

Bradbury, J. W. (1970). "Target discrimination by the echolocating bat, *Vampyrum spectrum*," *J. Exp. Zool.* **173**, 23–46.

Butler, R. A., and Belendiuk, K. (1977). "Spectral cues utilized in the localization of sound in the median sagittal plane," *J. Acoust. Soc. Am.* **61**, 1264–1269.

Calford, M. B., and Pettigrew, J. D. (1984). "Frequency dependence of directional amplification at the cat's pinna," *Hear. Res.* **14**, 13–19.

Carlile, S. (1990). "The auditory periphery of the ferret. I: Directional response properties and the pattern of interaural level differences," *J. Acoust. Soc. Am.* **88**, 2180–2195.

Carlile, S., and Pettigrew, A. G. (1987). "Directional properties of the auditory periphery in the guinea pig," *Hear. Res.* **31**, 111–122.

Casseday, J. H., and Covey, E. (1995). "Mechanisms for analysis of auditory temporal patterns in the brainstem of echolocating bats," in *Neural Representation of Temporal Patterns*, edited by E. Covey, H. L. Hawkins, and R. F. Port (Plenum, New York), pp. 25–51.

Dear, S. P., Fritz, J., Haresign, T., Ferragamo, M. J., and Simmons, J. A. (1993). "Tonotopic and functional organization in the auditory cortex of the big brown bat, *Eptesicus fuscus*," *J. Neurophysiol.* **70**, 1988–2009.

Djupestrand, G., and Zwislocki, J. J. (1973). "Sound pressure distribution in the outer ear," *Acta Oto-Laryngol.* **75**, 350–352.

Fisher, H., and Freedman, S. (1968). "The role of the pinna in auditory localization," *J. Aud. Res.* **8**, 15–26.

Flynn, W. E., and Elliott, D. M. (1965). "Role of the pinna in hearing," *J. Acoust. Soc. Am.* **38**, 104–105.

Griffin, D. R. (1958). *Listening in the Dark* (Yale U. P., New Haven CT; reprinted by Cornell U. P., Ithaca, NY, 1986).

Griffin, D. R. (1967). "Discriminative echolocation by bats," in *Animal Sonar Systems: Biology and Bionics*, edited by R.-G. Busnel (Laboratoire de Physiologie Acoustique, Jouy-en-Josas-78, France), pp. 273–300.

Guppy, A., and Coles, R. B. (1988). "Acoustical and neural aspects of hearing in the Australian gleaning bats, *Macroderma gigas* and *Nyctophylus gouldi*," *J. Comp. Physiol., A* **162**, 653–668.

Haberseizer, J., and Vogler, B. (1983). "Discrimination of surface-structured targets by the echolocating bat *Myotis myotis* during flight," *J. Comp. Physiol., A* **152**, 275–282.

Haplea, S., Covey, E., and Casseday, J. H. (1994). "Frequency tuning and response latencies at three levels in the brainstem of the echolocating bat, *Eptesicus fuscus*," *J. Comp. Physiol., A* **174**, 671–683.

Hebrank, J., and Wright, D. (1974). "Spectral cues used in the localization of sound sources in the median plane," *J. Acoust. Soc. Am.* **56**, 1829–1834.

Hiranaka, Y., and Yamasaki, H. (1983). "Envelope representations of pinna impulse responses relating to three-dimensional localization of sound sources," *J. Acoust. Soc. Am.* **73**, 291–296.

Jen, P. H.-S., and Chen, D. (1988). "Directionality of sound pressure transformation at the pinna of echolocating bats," *Hear. Res.* **34**, 101–118.

Kurta, A., and Baker, R. H. (1990). "*Eptesicus fuscus*," *Mammalian Species* **356**, 1–10.

Matsuo, I., Tani, J., and Yano, M. (2001). "A model of echolocation of multiple targets in 3D space from a single emission," *J. Acoust. Soc. Am.* **110**, 607–624.

Menne, D., and Hackbarth, H. (1986). "Accuracy of distance measurement in the bat *Eptesicus fuscus*: Theoretical aspects and computer simulations," *J. Acoust. Soc. Am.* **79**, 386–397.

Menne, D., Kaipf, I., Wagner, I., Ostwald, J., and Schnitzler, H.-U. (1989). "Range estimation by echolocation in the bat *Eptesicus fuscus*: trading of phase versus time cues," *J. Acoust. Soc. Am.* **85**, 2642–2650.

Middlebrooks, J. C. (1992). "Narrow-band sound localization related to external ear acoustics," *J. Acoust. Soc. Am.* **92**, 2607–2624.

Middlebrooks, J. C., and Green, D. M. (1991). "Sound localization by human listeners," *Annu. Rev. Psychol.* **42**, 135–159.

Mogdans, J., and Schnitzler, H. U. (1990). "Range resolution and the possible use of spectral information in the echolocating bat, *Eptesicus fuscus*," *J. Acoust. Soc. Am.* **88**, 754–757.

Moss, C. F., and Schnitzler, H.-U. (1995). "Behavioral studies of auditory information processing," in *Hearing by Bats*, edited by A. N. Popper and R. R. Fay (Springer-Verlag, New York), pp. 87–145.

Moss, C. F., and Simmons, J. A. (1993). "Acoustic image representation of a point target in the bat, *Eptesicus fuscus*: evidence for sensitivity to echo phase in bat sonar," *J. Acoust. Soc. Am.* **93**, 1553–1562.

Moss, C. F., and Surlykke, A. (2001). "Auditory scene analysis by echolocation in bats," *J. Acoust. Soc. Am.* **110**, 2207–2226.

Musicant, A. D., Chan, J. C. K., and Hind, J. E. (1990). "Direction-dependent spectral properties of cat external ear: New data and cross-species comparisons," *J. Acoust. Soc. Am.* **87**, 757–781.

Neuweiler, G. (2000). *The Biology of Bats* (Oxford U. P., New York).

Peremans, H., and Hallam, J. (1998). "The spectrogram correlation and transformation receiver, revisited," *J. Acoust. Soc. Am.* **104**, 1101–1110.

Phillips, D. P., Calford, M. B., Pettigrew, J. D., Aitkin, L. M., and Semple, M. N. (1982). "Directionality of sound pressure transformation at the cat's pinna," *Hear. Res.* **8**, 13–28.

Pollak, G. D. (1993). "Some comments on the proposed perception of phase and nanosecond time disparities by echolocating bats," *J. Comp. Physiol., A* **172**, 523–531.

Pollak, G. D., and Casseday, J. H. (1989). *The Neural Basis of Echolocation in Bats* (Springer, New York).

Popper, A. N., and Fay, R. R. (1995). *Hearing by Bats* (Springer, New York).

Rice, J. J., May, B. J., Spirou, G. A., and Young, E. D. (1992). "Pinna-based spectral cues for sound localization in cat," *Hear. Res.* **58**, 132–152.

Saillant, P. A. (1995). "Neural Computations for Biosonar Imaging in the Big Brown Bat," Ph.D. dissertation, Brown Univ. Graduate School, Providence, RI.

Saillant, P. A., Simmons, J. A., Dear, S. P., and McMullen, T. A. (1993). "A computational model of echo processing and acoustic imaging in frequency-modulated echolocating bats: The spectrogram correlation and transformation receiver," *J. Acoust. Soc. Am.* **94**, 2691–2712.

Sanderson, M. I., and Simmons, J. A. (2000). "Neural responses to overlapping FM sounds in the inferior colliculus of echolocating bats," *J. Neurophysiol.* **83**, 1840–1885.

Sanderson, M. I., and Simmons, J. A. (2002). "Selectivity for echo spectral shape and delay in the auditory cortex of the big brown bat, *Eptesicus fuscus*," *J. Neurophysiol.* (in press).

Schmidt, S. (1988). "Evidence for a spectral basis of texture perception in bat sonar," *Nature (London)* **331**, 617–619.

Schmidt, S. (1992). "Perception of structured phantom targets in the echolocating bat, *Megaderma lyra*," *J. Acoust. Soc. Am.* **91**, 2203–2223.

Schnitzler, H.-U., and Henson, O. W., Jr. (1980). "Performance of airborne

- animal sonar systems: I. Microchiroptera," in *Animal Sonar Systems*, edited by R.-G. Busnel and J. F. Fish (Plenum, New York), pp. 109–181.
- Schnitzler, H.-U., Menne, D., and Hackbarth, H. (1985). "Range determination by measuring time delays in echolocating bats," in *Time Resolution in Auditory Systems*, edited by A. Michelsen (Springer, Berlin), pp. 180–204.
- Shaw, E. A. G. (1982). "External ear response and sound localization," in *Localization of Sound: Theory and Applications*, edited by R. Gatehouse (Amphora, Groton, CT), pp. 30–41.
- Shaw, E. A. G., and Teranishi, R. (1968). "Sound pressure generated in an external-ear replica and real human ears by a nearby sound source," *J. Acoust. Soc. Am.* **44**, 240–249.
- Simmons, J. A. (1973). "The resolution of target range by echolocating bats," *J. Acoust. Soc. Am.* **54**, 157–172.
- Simmons, J. A. (1979). "Perception of echo phase information in bat sonar," *Science* **204**, 1336–1338.
- Simmons, J. A. (1980). "The processing of sonar echoes by bats," in *Animal Sonar Systems*, edited by R.-G. Busnel and J. F. Fish (Plenum, New York), pp. 695–714.
- Simmons, J. A. (1982). "The external ears as receiving antennae in echolocating bats," *J. Acoust. Soc. Am. Suppl. 1* **72**, S41–S42.
- Simmons, J. A. (1989). "A view of the world through the bat's ear: The formation of acoustic images in echolocation," *Cognition* **33**, 155–199.
- Simmons, J. A. (1993). "Evidence for perception of fine echo delay and phase by the FM bat, *Eptesicus fuscus*," *J. Comp. Physiol., A* **172**, 533–547.
- Simmons, J. A. (1996). "Formation of perceptual objects from the timing of neural responses: Target-range images in bat sonar," in *The Mind-Brain Continuum: Sensory Processes*, edited by R. Llinás and P. S. Churchland (MIT, Cambridge, MA), pp. 219–250.
- Simmons, J. A., and Chen, L. (1989). "The acoustic basis for target discrimination by FM echolocating bats," *J. Acoust. Soc. Am.* **86**, 1333–1350.
- Simmons, J. A., and Grinnell, A. D. (1988). "The performance of echolocation: Acoustic images perceived by echolocating bats," in *Animal Sonar: Processes and Performance*, edited by P. Nachtigall and P. W. B. Moore (Plenum, New York), pp. 353–385.
- Simmons, J. A., Eastman, K. M., and Horowitz, S. S. (2001). "Versatility of biosonar in the big brown bat, *Eptesicus fuscus*," *Acoustics Research Letters Online* **2**, 43–48.
- Simmons, J. A., Ferragamo, M. J., and Moss, C. F. (1998). "Echo-delay resolution in sonar images of the big brown bat, *Eptesicus fuscus*," *Physica A* **95**, 12647–12652.
- Simmons, J. A., Moss, C. F., and Ferragamo, M. (1990a). "Convergence of temporal and spectral information into acoustic images of complex sonar targets perceived by the echolocating bat, *Eptesicus fuscus*," *J. Comp. Physiol., A* **166**, 449–470.
- Simmons, J. A., Saillant, P. A., and Dear, S. P. (1992). "Through a bat's ear," *IEEE Spectrum* March, 46–48.
- Simmons, J. A., Ferragamo, M. J., Moss, C. F., Stevenson, S. B., and Altes, R. A. (1990b). "Discrimination of jittered sonar echoes by the echolocating bat, *Eptesicus fuscus*: The shape of target images in echolocation," *J. Comp. Physiol., A* **167**, 589–616.
- Simmons, J. A., Freedman, E. G., Stevenson, S. B., Chen, L., and Wohlgenant, T. J. (1989). "Clutter interference and the integration time of echoes in the echolocating bat, *Eptesicus fuscus*," *J. Acoust. Soc. Am.* **86**, 1318–1332.
- Simmons, J. A., Ferragamo, M. J., Saillant, P. A., Haresign, T., Wotton, J. M., Dear, S. P., and Lee, D. N. (1995). "Auditory dimensions of acoustic images in echolocation," in *Hearing by Bats*, edited by A. N. Popper and R. R. Fay (Springer-Verlag, New York), pp. 146–190.
- Simmons, J. A., Saillant, P. A., Ferragamo, M. J., Haresign, T., Dear, S. P., Fritz, J., and McMullen, T. A. (1996). "Auditory computations for biosonar target imaging in bats," in *Auditory Computation*, edited by H. L. Hawkins, T. A. McMullen, A. N. Popper, and R. R. Fay (Springer-Verlag, New York), pp. 401–468.
- Simmons, J. A., Lavender, W. A., Lavender, B. A., Doroshov, D. A., Kiefer, S. W., Livingston, R., Scallet, A. C., and Crowley, D. E. (1974). "Target structure and echo spectral discrimination by echolocating bats," *Science* **186**, 1130–1132.
- Wightman, F. L., and Kistler, D. J. (1989). "Headphone simulation of free-field listening. I: Stimulus synthesis," *J. Acoust. Soc. Am.* **85**, 858–867.
- Wotton, J. M., Haresign, T., and Simmons, J. A. (1995). "Spatially dependent acoustic cues generated by the external ear of the big brown bat, *Eptesicus fuscus*," *J. Acoust. Soc. Am.* **98**, 1423–1445.
- Wotton, J. M., Jenison, R. L., and Hartley, D. J. (1997). "The combination of echolocation emission and ear reception enhances directional spectral cues of the big brown bat, *Eptesicus fuscus*," *J. Acoust. Soc. Am.* **101**, 1723–1733.
- Wotton, J. M., Haresign, T., Ferragamo, M. J., and Simmons, J. A. (1996). "The influence of sound source elevation and external ear notch cues on the discrimination of spectral notches by the big brown bat, *Eptesicus fuscus*," *J. Acoust. Soc. Am.* **100**, 1764–1776.
- Wright, D., Hebrank, J. H., and Wilson, B. (1974). "Pinna reflections as cues for localization," *J. Acoust. Soc. Am.* **56**, 957–962.